

The following article is hosted by PTB;

DOI: 10.7795/810.20251001 It is provided for personal use only.

FEM analysis of thermal properties of an optical gas cell for ro-vibrational spectroscopic thermometry

Kianoosh Hadidi, Gang Li

Acknowledgement: This work was supported by the EURAMET Metrology Partnership project “PriSpecTemp” [grant numbers 22IEM03] titled “Primary Spectrometric Gas Thermometry”. This project has received funding from Metrology Partnership programme co-financed by the Participating States and the European Union's Horizon 2020 research and motivation programme.

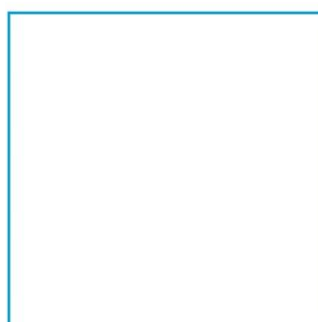
Available at:

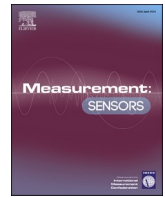
Originally published at:

<https://doi.org/10.1016/j.measen.2024.101639>

License:

[CC-BY 4.0](https://creativecommons.org/licenses/by/4.0/)





FEM analysis of thermal properties of an optical gas cell for ro-vibrational spectroscopic thermometry

ARTICLE INFO

Keywords:

Optical cell
Temperature gradient
Finite element method

ABSTRACT

We utilised Finite Element Method (FEM) to analyse the thermal behaviour of newly designed optical gas cell. We have investigated the impact of the gas pressure, design of the optical windows, thermal radiation and the flow regime inside the heat exchanger on the temperature gradient in the spectroscopic gas cells. Considering practical spectroscopic measurement conditions, the simulation covered wide ranges of pressure and temperature, from 1 mbar to 1000 mbar, and from 200 K to 400 K, respectively. The results of the FEM analysis highlight the significance of the design of optical windows, including the size and isolation, in maintaining gas thermodynamic stability and homogeneity. Moreover, the simulation demonstrates how temperature profiles vary in different conditions and how viscous dissipation in the heat exchanger fluid affects the gas temperature uniformity. Furthermore, the study emphasises the importance of the place where the temperature sensor is installed, for accurate temperature measurement. The findings of this research aim to provide valuable insights for the future design of optical gas cells.

1. Introduction

Gas cells are commonly used in optical gas analysers employed to determine the amount fraction of target molecules in a gas sample [1], gas temperature [2], and isotope ratio [3]. Despite the successful thermal design of laser-based Doppler thermometry [4], ro-vibrational spectroscopic thermometers [5] require improvement in the gas cell design and characterisation of its thermal properties. A significant challenge arises from the non-uniform temperature distribution inside the gas cells, posing the risk of large uncertainties in measured temperatures. This issue stems from various factors, including structural deficiencies and the specific design of the gas cell's heat treatment. For instance, a well-recognized problem in this context is the temperature disparity near the optical windows, given their direct contact with the ambient temperature.

Compounding the challenge is the absence of precise knowledge regarding temperature distribution within the gas because of the technical complexities associated with direct temperature measurements. Typically, the measured temperature at a point external to the gas cell body is conventionally considered the reference for the gas temperature. However, recognising the limitations of this approach, simulation offers a clear understanding of the thermal dynamics within the gas cell, allowing for a thorough assessment and optimization of the optical cell design. In this study, we have tried to address the thermodynamic pattern at different conditions to identify how to reduce the potential uncertainties in spectroscopic thermometry.

This work is part of the PriSpecTemp (Primary Spectrometric Thermometry for Gases) project [6], which aims to achieve an accuracy level of 25 mK or better in thermodynamic temperature using ro-vibrational spectroscopic gas thermometry (RVSGT). In support of this goal, the present simulation study was conducted as a prerequisite for designing

an optical cell, with an uncertainty target of 10 mK in temperature measurement.

2. Methods

We employed Comsol Multiphysics simulation software for our analysis. The heat exchanger system which contains silicon oil surrounds the gas cell and adopts a labyrinth form to facilitate heat transfer to both sides of the gas cell body simultaneously (Fig. 1). This system is utilised for both cooling and heating the gas cell. Silicon oil allows to cover a temperature range of 200–400 K without the system undergoing a phase change. Air is the gas inside the cell.

The relevant tolerance for the calculations was set to 0.1 mK to ensure accuracy on the order of milli kelvins. The temperature inhomogeneity in the gas was analysed in terms of heat transfer to the ambient environment through the optical windows, in combination with pressure. The rest of the system has been kept in adiabatic condition, considering that the outermost walls are isolated. Two different models for the optical cell were designed. In the first model (Fig. 2b) the optical windows are in direct contact with the ambient conditions. In the second model (Fig. 2a) a vacuum housing surrounds the gas cell, where, in addition to the other mechanisms of heat transfer, radiation has also been considered for the transparent and environments.

The diameters of the vacuum house, optical windows, gas cell and heat exchanger spiral are 20 cm, 2.4 cm, 9 cm and 1.6 cm respectively. The length of the gas cell, heat exchanger system and vacuum housing are 21.6, 22.4 and 56 cm respectively. Gravity was oriented along the y-axis to model a horizontal cell. However, the vertical model was also examined to explore potential differences in the thermodynamic approach within the two cell designs. No significant differences were identified between the two designs in the simulation.

<https://doi.org/10.1016/j.measen.2024.101639>

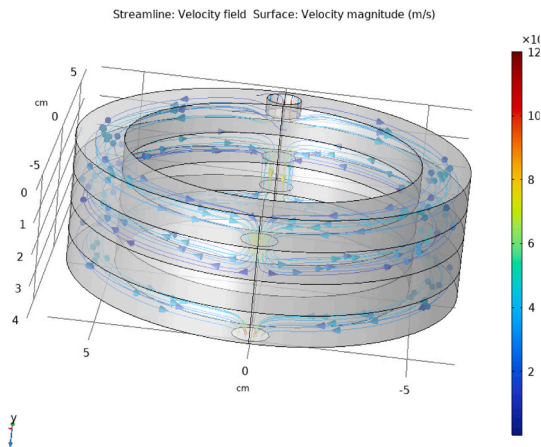


Fig. 1. The fluid system around the gas cell which provides the temperature adjustment. The blue arrows represent the flow direction. The fluid fills both sides of the cell simultaneously, ensuring more uniform temperature distribution.

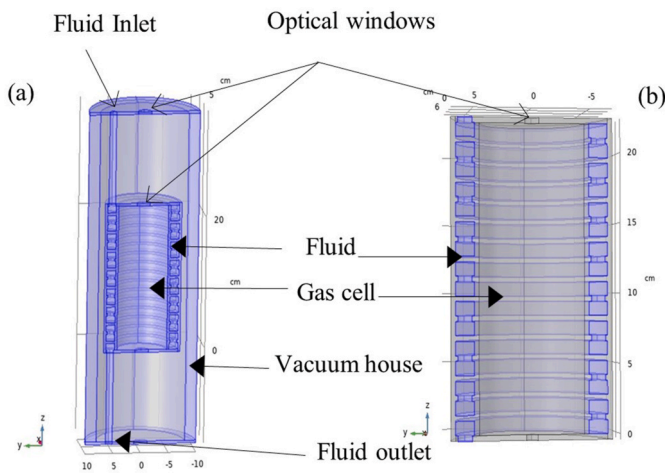


Fig. 2. (a) optical cell with vacuum housing. Optical windows at both sides of the optical cell are in direct contact with the ambient condition. Heat transfer through vacuum occurs by thermal radiation. (b) The optical windows on the gas cell are in direct contact with ambient environment.

Fig. 3 represents the paths within the gas cell where we observed the temperature distribution: lines extending from the beginning to the end of the gas cell, distributed along the diameter in y -direction. This option provides us with the possibility to investigate the temperature gradient along the direction of gravity, while accounting for the proximity to both the optical windows and the fluid inlet of the gas cell. We consider that

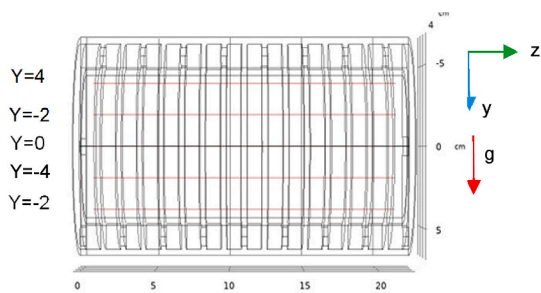


Fig. 3. Paths for temperature monitoring extended from the top to the end of the gas cell and distributed along the diameter in the y -axis corresponding to gravity direction.

the other regions of the gas cell have symmetrically the same conditions.

3. Results and discussion

The area close to the ambient environment, such as optical windows are particularly sensitive to temperature gradients as it is difficult to completely isolate them from the surrounding environment. **Fig. 4** illustrates the temperature gradient along the paths shown in **Fig. 3**, which corresponds to the gas cell directly exposed to the ambient environment via optical windows. The inlet temperature of the fluid is 400 K. The analysis was conducted in air at different pressures, namely 1, 500 and 1000 mbar. The initial temperature of the silicon oil at the heat exchanger inlet is 400 K. At 1 mbar pressure, there is a temperature difference of 17 K between the area near the optical windows and the centre of the gas cell along the central path ($y = 0$). In this system, the gas pressure inside the gas cell influences the temperature distribution, resulting in higher temperatures at higher pressures. The maximum temperature variation for 500 mbar is around 9.5 K which is observed between the similar points as described for 1 mbar. This significant temperature variation is shown at 400 K. It will naturally decrease at lower gas temperatures. Nevertheless, this serves as a clear demonstration of the importance of reducing the contact area between the optical window and ambient conditions. The use of a vacuum housing (**Fig. 2a**) can significantly decrease the thermal interaction of the gas cell with the surrounding environment. However, heat still transfers through radiation from the gas cell to the body and optical windows of the vacuum housing, as illustrated in **Fig. 5a** and **b** for temperatures of 200 K and 400 K, respectively.

The model with vacuum housing was examined under both laminar and turbulent flow conditions of the silicon oil inside the heat exchanger. The suitable velocities for modelling each flow regime were determined by applying the properties of the silicon oil at the specified temperature in the Reynolds number equation. As a result of this calculation, velocities of 0.1 m/s and 0.5 m/s were employed for the laminar and turbulent regimes at 400 K. Similarly, velocities of 0.5 m/s and 2 m/s were utilised to simulate the laminar and turbulent flow regimes at 200 K. The temperature profile for laminar flow at 400 K and 1 mbar, as depicted in **Fig. 6a**, demonstrates a 20 times greater temperature range than that for turbulent flow along the central line $y = 0$. Specially the laminar flow shows a variation of about 0.6 K, whereas turbulent flow indicates a variation of around 30 mK. There is a maximum temperature difference of 40–70 mK between corresponding points in **Fig. 6a** and **b**, indicating lower temperatures inside the gas cell with surrounding laminar flow compared to turbulent flow. This is expected as thermal interaction is more effective in turbulent flow. The gas

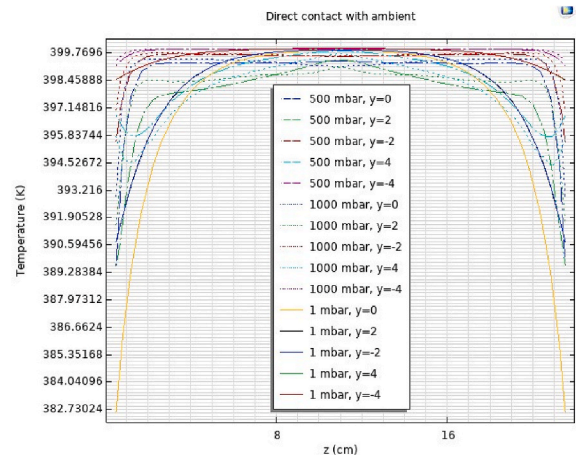


Fig. 4. Temperature distribution in the gas cell with the direct contact with the ambient conditions. The fluid temperature at the heat exchanger inlet is 400 K.

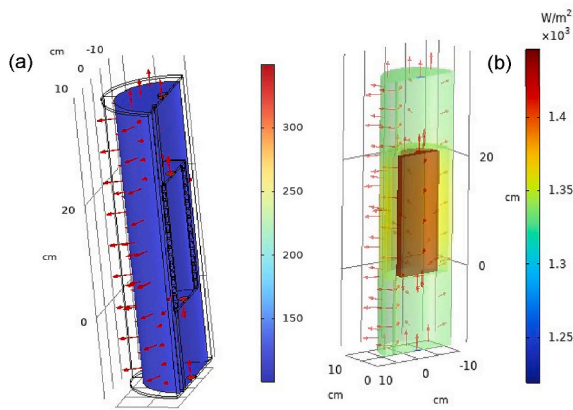


Fig. 5. Illustration of thermal radiation from the gas cell to the vacuum housing (a) at 200 K (b) at 400 K.

temperature difference from the heat exchanger changes from 121 to 61 mK for the laminar flow and from 64 mK to 11 mK for turbulent flow on the central path $y=0$. In comparison the paths on the sides of the optical windows show a maximum difference of 15 mK for 400 K. At the lower gas pressure, the system with laminar flow shows a higher temperature difference from the temperature of the heat exchanger.

Fig. 7 exhibits the temperature non-uniformity inside the gas cell at 200 K. It presents a higher temperature than 200 K on the central line ranging from 14 to 16 mK difference for laminar flow and 28–45 mK difference for turbulent flow. For laminar regime with the silicon oil velocity of 0.5 m/s, the gas temperature near the optical windows to the gas cell ($z = 0$) is higher compared to other areas as expected. The temperature difference between the two ends of the gas cell is more pronounced at 200 K compared to 400 K, and is on the order of 5 mK. There is also temperature dispersion close to the fluid inlet, while the temperatures along different paths, except for the central path, converge together for both 1 and 1000 mbar towards the end of the gas cell. Temperature profile at Fig. 7b for turbulent flow exhibits a special shape. The temperature begins to escalate continuously from a short distance from the optical window towards the end of the gas cell, leading to a higher temperature of approximately 10 mK. This behaviour is attributed to the viscous dissipation resulting from turbulent flow

coupled with the higher dynamic viscosity of silicon oil at this temperature.

Another challenge for accurate temperature measurement of the gas in spectroscopic setups is the limitation on using intrusive methods. The temperature sensors are usually installed outside the gas cell and at the first body which surrounds it. Thus, we do not obtain a precise knowledge of the temperature within the gas cell. This can lead to additional uncertainty in temperature measurement. We have simulated a vacuum housing around the gas cell which is affected by the gas temperature through radiation. Fig. 8 is an illustration of the potential difference between the measured temperature on the surrounding body and the gas temperature. It is seen that the temperature at the vacuum housing is not uniform. It presents a gradient in terms of the distance from the fluid inlet and outlet on the body and optical windows. At 400 K, the temperature variation is on the order of 300 mK and 0.060 mK for laminar and turbulent flow respectively. This value is on the order of 64 mK and 24 mK for the two flow regimes at 200 K. The temperature range on the vacuum house body is over 1 K lower compared to the minimum and maximum temperatures on the central path inside the gas cell for both flow regimes at 400 K. This difference is 0.35 K and 0.6 K for turbulent and laminar flow under the same comparison at 200 K.

4. Conclusions

We have developed two optical cell models to address the issue of temperature non-uniformity within gas cells in spectroscopy setups, as well as temperature disparities between the interior and exterior of the gas cell. Our findings demonstrate that the most significant non-uniformity inside the gas cell occurs when there are direct contacts with the ambient environment, such as at optical windows. Even in cases of indirect contact with ambient conditions through a vacuum space, the gas cell still exhibits a temperature gradient ranging from 14 to 70 mK. In the model where temperature regulation is performed by a heat exchanger, the influential parameters on the temperature gradient are identified as gas pressure, flow regime inside the heat exchanger, fluid viscosity (which is temperature-dependent), and the size and design of the optical windows. It was also shown that the installation place of the temperature sensors can potentially lead to significant uncertainties.

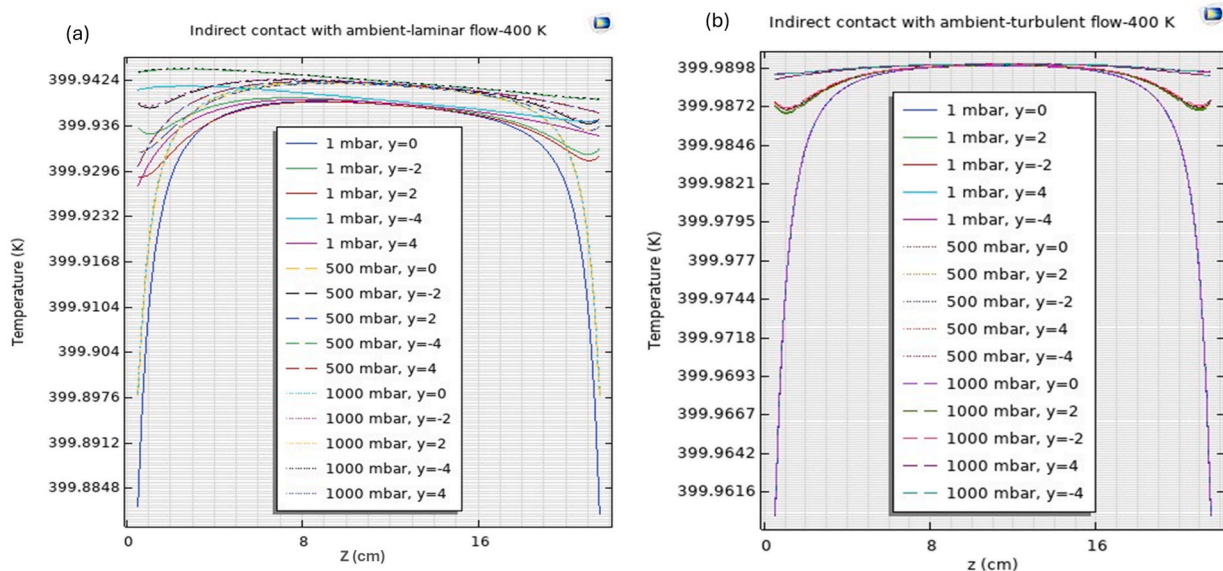


Fig. 6. Temperature distribution for the gas cell shown in Fig. 2a, where the fluid temperature at the heat exchanger inlet is 400 K (a) for laminar flow regime (b) for turbulent flow regime in the silicon oil.

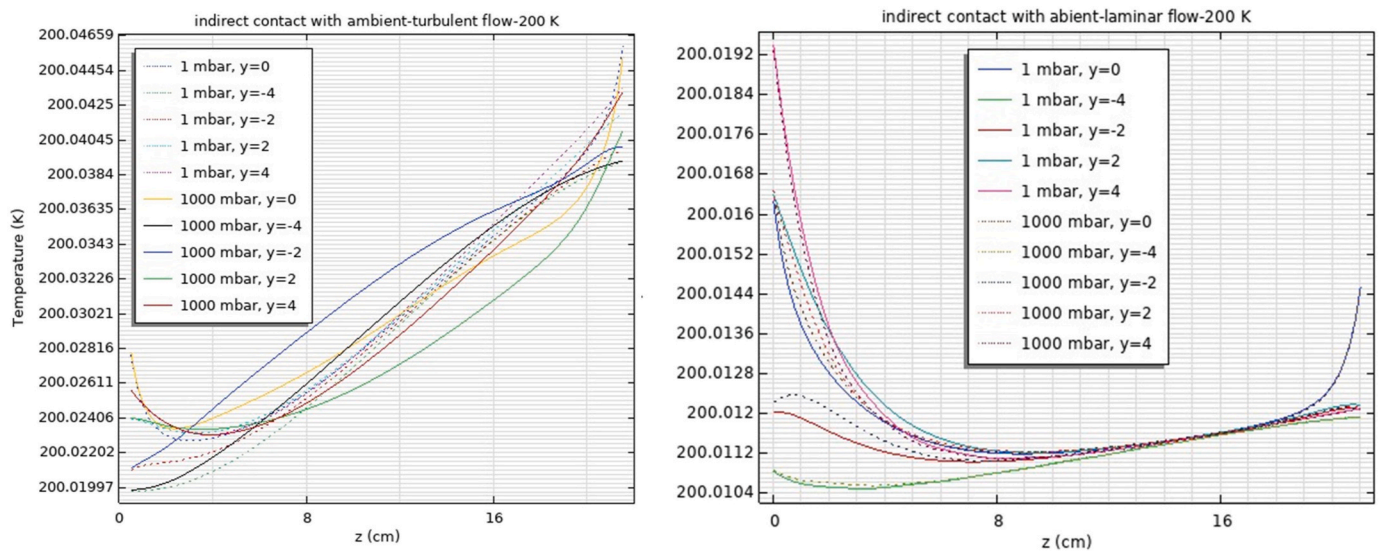


Fig. 7. Temperature distribution for the gas cell shown in Fig. 2a, where the fluid temperature at the heat exchanger inlet is 200 K (a) for laminar flow regime (b) for turbulent flow regime in the silicon oil.

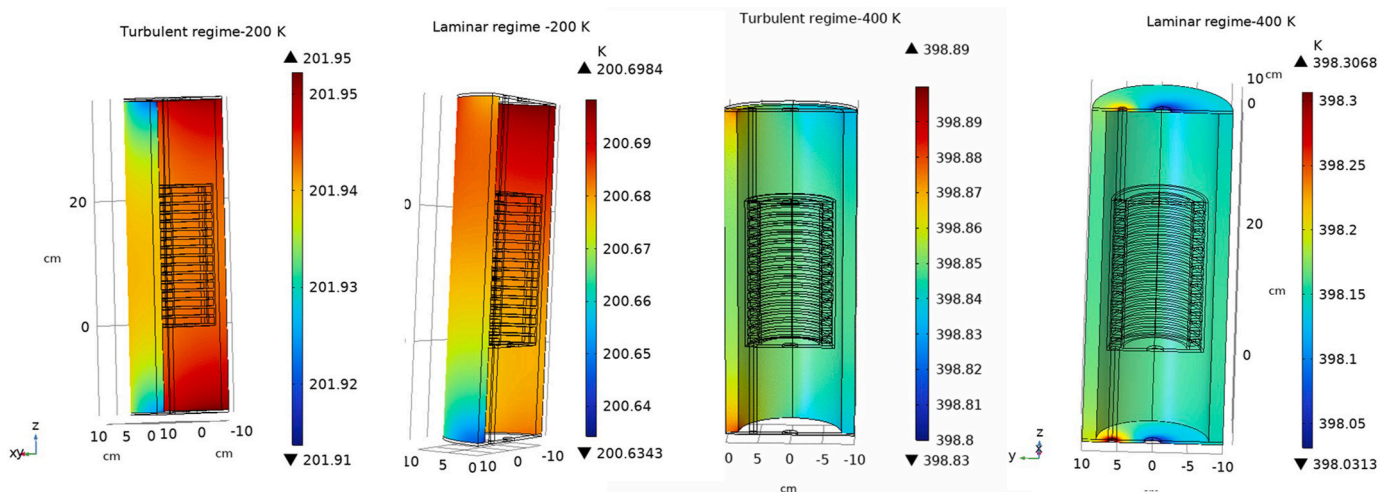


Fig. 8. Temperature distribution at the vacuum housing at 200 K and 400 K for laminar and turbulent flow regimes in the heat exchanger.

Funding statement

This work was supported by the EURAMET Metrology Partnership project “PriSpecTemp” [grant numbers 22IEM03]. This project has received funding from Metrology Partnership programme co-financed by the Participating States and the European Union’s Horizon 2020 research and motivation programme.

Acknowledgments

We are much obliged to E. Kristiansen at Comsol Support Center for the invaluable technical support.

References

- [1] Paul V. Torek, David L. Hall, Tiffany A. Miller, Margaret S. Wooldrige, H₂O absorption spectroscopy for determination of temperature and H₂O mole fraction in high-temperature particle synthesis systems, *Appl. Opt.* 41 (12) (2002) 2274–2284, <https://doi.org/10.1364/AO.41.002274>.
- [2] G. Casa, A. Castrillo, G. Galzerano, R. Wehr, A. Merlone, D. Di Serafino, P. Laporta, L. Gianfrani, Primary gas thermometry by means of laser-absorption spectroscopy:

- determination of the Boltzmann constant, *Phys. Rev. Lett.* 100 (2008) 200801, <https://doi.org/10.1103/PhysRevLett.100.200801>.
- [3] I. Prokhorov, T. Kluge, C. Janssen, Optical clumped isotope thermometry of carbon dioxide, *Sci. Rep.* 9 (2019) 4765, <https://doi.org/10.1038/s41598-019-40750-z>.
- [4] A. Merlone, F. Moro, A. Castrillo, L. Gianfrani, Design and capabilities of the temperature control system for the Italian experiment based on precision laser spectroscopy for a new determination of the Boltzmann constant, *Int. J. Thermophys.* 31 (2010) 1360–1370, <https://doi.org/10.1007/s10765-010-0728-6>.
- [5] Gang Li, Volker Ebert, *Broadband Rovibrational Spectroscopic Thermometry for Gases*, TEMPMEKO2019, 2019. Chengdu, China.
- [6] EURAMET Metrology Partnership project “22IEM03 PriSpecTemp”. <https://www.prispectemp.ptb.de/home>.

Kianoosh Hadidi^{a,*}, Gang Li^b

^a National Laboratory, Norwegian Metrology Service (JV), Fetveien 99, 2007, Kjeller, Norway

^b Physikalisch-Technische Bundesanstalt (PTB), Braunschweig, Germany

* Corresponding author.

E-mail addresses: kih@justervesenet.no (K. Hadidi), gang.li@ptb.de (G. Li).